# PERFORMANCE PREDICTION AND DESIGN OPTIMIZATION OF A kW-SIZE RECIPROCATING PISTON EXPANDER WORKING WITH LOW-GWP FLUIDS

M. A. Ancona, M. Bianchi, L. Branchini*, A. De Pascale, F. Melino, S. Ottaviano, A. Peretto, N. Torricelli

Department of Industrial Engineering
Alma Mater Studiorum – University of Bologna, Italy
e–mail: lisa.branchini2@unibo.it

* Corresponding Author

## ABSTRACT

Micro-ORC systems represent a promising technology in the field of the energy conversion from low-grade temperature sources. However, nowadays the working efficiency are still relatively low, resulting from the lack of appropriate expander machines but also from the need of optimal working fluid. The ideal working fluid should maximize the performance of the system for given operating conditions (as the hot source temperature) and, at the same time, it must respect the environmental impact restrictions, linked to the fluid ozone depletion potential (ODP) and global warming potential (GWP). In this study, low-GWP fluids, as R1234yf and R1234ze(E) have been compared with R134a, as working fluid of a kW-size reciprocating piston expander and the optimization of the built-in volume ratio has been performed for each analyzed fluid in design conditions. To this purpose, a previously calibrated and validated semi-empirical model of the expander has been integrated with a new gear pump model, in order to simulate the volumetric machines into the real operation of the ORC system. The comprehensive model is conceived to accommodate the change of the working fluid: model parameters taking into account the thermo-fluid-dynamic properties of the fluid are updated compared to the original values calibrated over R134a by means of an extensive experimental campaign.

## 1. INTRODUCTION

The Organic Rankine Cycle (ORC) technology, as waste heat recovery system, can represent a substantial contribution for saving primary sources and emissions, within the distributed generation concept. However, although ORC is a mature technology for the medium-to-large size, very few ORC plants exist in the kW power range (Quoilin *et al*., 2013). Focusing on micro size, the working efficiency are still relatively low, resulting from the lack of appropriate expander machines in the commercial market but also from the need of optimal working fluid for low temperature applications (Qiu, 2012).

Nowadays, expanders for micro-size applications are still in-house designed and manufactured, mostly at prototypal level (Quoilin *et al*., 2013). In order to evaluate the performance of such expanders in a real heat recovery application, it can be useful to simulate their behavior in specific operating conditions that can differ from the design point considered by the manufacturer. Models of semi-empirical type can be the best choice, since they offer a good trade-off between simulation speed, calibration efforts, modelling accuracy and extrapolation capability (Dumont *et al*., 2017). The other most important degree of freedom in the design of an ORC cycle is the choice of the proper working fluid: the fluid impacts the thermodynamic cycle, the cost of the components, the safety requirements and the environmental impact (Qiu, 2012). Indeed, refrigerants pose a threat to the environment because of their ozone depletion potential (ODP) and global warming potential (GWP), and in recent decades, a series of legislations have been introduced in order to control their use, as the Montreal Protocol in 1989 and the EU MAC directive 2006/40 in 2006. Concerning low temperature applications (temperatures lower than 150 °C) one of the most suitable working fluid for small-scale ORC is the HFC-134a. As most promising substitutive low GWP fluids the HFO-1234yf and the

HFO-1234ze(E) have been identified. Despite they have been already introduced in some car air-conditioning systems and are commercially available for use in centrifugal chillers, they still need to be extensively tested into expander machines for ORC applications. In this context, different studies have investigated the performance of the HFOs as substitutes of R134a into ORC cycles (Yamada *et al*., 2012) (Le *et al*., 2014) (Molés *et al*., 2017).
A kW size ORC test rig, driven by a reciprocating piston expander prototype, has been developed at the Laboratory of the University of Bologna for performance analysis. In previous works the expander and the whole system has been tested for a wide range of operating conditions, fed with R134a (Bianchi *et al*., 2019a); a semi-empirical model has been implemented, calibrated and validated versus the available experimental data, in order to simulate the prototypal expander of the case study over an extended range of operating conditions (Bianchi *et al*., 2019b). The objective of this study is to use the validated expander model to simulate its performance in case of replacing R134a with its low-GWP alternative fluids. With this purpose, the original model (based on the work of Glavatskaya *et al*., 2012) has been modified with the procedure proposed by Giuffrida (2014) to be used with fluids other than R134a. In this work the Authors introduce a semi-empirical model of the gear pump to be integrated with the expander one, with the aim of predicting the expander performance in its real operation into the actual cycle. Models parameters related to thermo-fluid-dynamic properties were updated compared to the original calibrated and validated values over R134a. The integrated model allows to predict the performance of the volumetric expander using low-GWP working fluids and to identify the optimal built-in volume ratio to maximize the electric power output in design conditions.

## 2. THE EXPERIMENTAL SETUP

The ORC test bench is conceived for exploiting low-grade heat sources, with temperatures lower than 100 °C in the kW range of power. The key component of the system is a prototypal reciprocating expander developed by the StarEngine company. The expander consists in three cylinders placed radially at 120°, with a total displacement equal to 230 $cm^3$. The admission and the discharge of the vapor at the expander are executed by rotatory valves, that are placed in correspondence of the cylinder head and are driven by the crankshaft rotation, see Bianchi *et al*., 2019a. The expander is directly coupled with the generator, which is connected to an electrical load, made of five pure resistive loads, connected in parallel between them and in delta with the generator output three-phase line. In this configuration, the load does not allow setting the generator rotational speed nor the load torque, and the expander shaft is free to achieve the equilibrium between the generator torque and the set load resistance. The other components of the circuit are the evaporator and a recuperator, a condenser and a volumetric gear pump with frequency drive (gear ratio 3:1), which allows a proper regulation of the flow rate of the working fluid, since the pump is of positive displacement type. The ORC circuit is currently using, as working fluid, Freon R134a. The test bench is then fully equipped with an acquisition system. In order to collect data in specific testing conditions, four main parameters can be controlled from the outside: the water temperature at the evaporator inlet ($T_{H2OhotIN}$), the water temperature at the condenser inlet ($T_{H2OcoolingIN}$), the feed pump frequency ($f_{pump}$) and the number of activated resistive loads ($n_{loads}$). For further information, consult the work of the Authors (Bianchi *et al*., 2019a), which presents a complete description of the test-rig, acquisition system and the extensive experimental campaign performed on the micro-ORC system.

## 3. THE MODEL

The model has been implemented in the Matlab environment and the thermodynamic properties of the fluids have been calculated by means of the CoolProp library (Bell *et al.*, 2014)..

### 3.1 Integrated model

The pump and the expander semi-empirical sub-models (detailed in the following paragraphs) have been integrated into a comprehensive calculation code routine shown in Figure 1, with the purpose of simulating the expander behavior in its real operation into the cycle. The inputs of the integrated model are the control variables of the system ($T_{H2OhotIN}$, $T_{H2OcoolingIN}$, $f_{pump}$ and $n_{loads}$): this choice allows performing a fair comparison of the performance of the system when changing working fluid,

considering the same temperature of the hot and the cold sources, the same pump frequency and the same system resistance. The condensation temperature determines the condensation pressure of the cycle ($p_{ex}$), assumed to be equal to the saturation pressure at the condensation temperature. The hot source temperature, instead, determines the expander inlet temperature ($T_{su}$), assumed to be equal to the hot source temperature minus a temperature delta ($\Delta T$) at the evaporator. The pump model requires as input the frequency of the pump, the number of activated resistive loads and the condensation pressure, to give as output the mass flow rate, $\dot{m}$, and the pump downstream pressure, $p'_{su}$. The expander inlet pressure ($p_{su}$) is computed by subtracting to $p'_{su}$ a pressure drop term, $\Delta p_{loss}$, representing the pressure drop that occurs between the pump outlet and the expander inlet. The organic fluid mass flow rate at the outlet of the pump is equal to the mass flow rate that enters into the expander, in steady-state conditions. The organic fluid mass flow rate and the evaporation pressure, together with the temperature at the inlet of the expander and the condensation pressure, are the inputs of the expander model. The outputs of the expander model coincide with the outputs of the integrated model i.e. the shaft rotational speed of the expander ($N_{exp}$), the electric power output ($\dot{W}_{el}$) and the expander outlet temperature ($T_{ex}$).

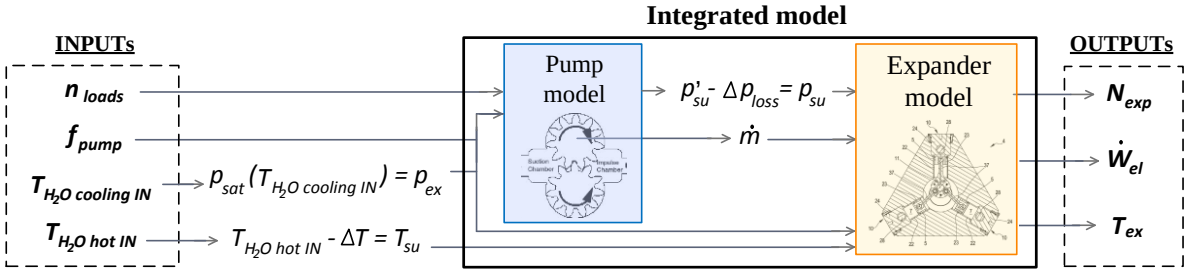


**Figure 1:** Inputs and outputs of the integrated model.

### 3.2 Reciprocating expander model

The selected model has been originally proposed by Glavatskaya *et al.* (2012) and then adapted, calibrated and validated versus experimental data for the reciprocating expander of the case study. For more details about the model equations and the implemented calibration process, the reader is referred to the previous work of the Authors (Bianchi *et al*., 2019b). The model is a semi-empirical lumped parameters model, since it relies on a number of physical equations containing some empirical parameters, which must be calibrated by interpolating the experimental data. In particular, the equations of the model are based on the scheme and the p-V diagram shown in Figure 2. A summary of the input, output, constant values and calibrated model parameters is provided in Table 1.

### 3.3 Correction of the heat transfer parameters of the expander model

In this study, in order to predict the performance of the expander when substituting the working fluid, the parameters accounting for the thermo-fluid-dynamic properties, have been re-determined, adopting the procedure proposed by Giuffrida (2014). The parameters to be corrected are $(AU)_{su,ref}$ and $(AU)_{ex,ref}$ used to model the heat transfer between the working fluid and the casing, respectively before and after the internal expansion. The thermal transmittance, $U$ , is evaluated as:

$$U = \frac{Nu \cdot \lambda}{L} \tag{1}$$

where $Nu$ is the Nusselt number, $\lambda$ is the conductivity and $L$ is the characteristic length. The Nusselt number is calculated using the Dittus-Boelter correlation for turbulent flows:

$$Nu = 0.023 \cdot \mathrm{Re}^{0.8} \cdot \mathrm{Pr}^{m} \tag{2}$$

with $m$ = 0.4 if the fluid is heated by the wall; otherwise, if the fluid is cooled by the wall, $m$ = 0.3. Given that the characteristic length is set and the velocity does not depend on the working fluid (being set the flow passage area and the swept volume), the global heat transfer parameter for the new fluid, $(AU)_{ref,fluid}$, can be determined by manipulating equation (3).

$$\frac{(AU)_{ref,fluid}}{(AU)_{ref,R134a}} = \frac{Nu_{fluid} \cdot \lambda_{fluid}}{Nu_{R134a} \cdot \lambda_{R134a}} \tag{3}$$

$$(AU)_{ref,fluid} = (AU)_{ref,R134a} \cdot \left(\frac{\rho_{fluid}}{\rho_{R134a}}\right)^{0.8} \cdot \left(\frac{c_{pfluid}}{c_{pR134a}}\right)^{m} \cdot \left(\frac{\lambda_{fluid}}{\lambda_{R134a}}\right)^{1-m} \cdot \left(\frac{\mu_{R134a}}{\mu_{fluid}}\right)^{0.8-m} \tag{4}$$

where $\rho$ is the fluid density, $c_p$ is the heat capacity at constant pressure and $\mu$ the fluid viscosity; the subscript *fluid* indicates the quantities related to the new fluid, while the subscript *R134a* indicates the quantities related to R134a. Equation (4) is applied to both the parameters $(AU)_{su,ref}$ and $(AU)_{ex,ref}$. The thermodynamic properties of the fluids included into equation (4) have been evaluated in the design operating point: the reference state for the parameter $(AU)_{su,ref}$ is defined by a pressure of 15 bar and a temperature of 75 °C, while the reference state for $(AU)_{ex,ref}$ is defined by a pressure of 7 bar and a temperature of 50 °C. The resulting corrected parameters are listed below in Table 2.

**Table 1:** Summary of the input, output, constant values and models calibration parameters.

| **Inputs** | **Model parameters** | | **Calibrated value** | | **Outputs** |
|---|---|---|---|---|---|
| $T_{su}$ | $(AU)_{su,ref}$ | Supply heat transfer coefficient | 5.65e-05 | (W/K) | $T_{ex}$ |
| $p_{su}$ | $(AU)_{ex,ref}$ | Exhaust heat transfer coefficient | 9.23e-05 | (W/K) | $N_{exp}$ |
| $p_{ex}$ | $(AU)_{amb}$ | Ambient heat transfer coefficient | 0.96 | (W/K) | $\dot{W}_{el}$ |
| $\dot{m}$ | $r_{v,exp}$ | Built-in volume ratio | 1.459 | - | |
| | $r_{v,comp}$ | Re-compression volume ratio | 1.25 | - | |
| **Constants** | $V_0$ | Clearance volume | 2.32e-02 | ($cm^3$) | |
| Swept volume $Vs$ = 230 $cm^3$, | $A_{leak}$ | Equivalent leakage area | 5.51e-06 | ($m^2$) | |
| Electro-mechanical conversion efficiency = 90 % | $A_{su}$ | Supply nozzle equivalent section | 1.47e-05 | ($m^2$) | |
| | $W_{loss,ref}$ | Constant friction losses | 0.198 | (W) | |
| | $W_{loss,N}$ | Proportional friction losses | 1.07e-05 | (W/min) | |

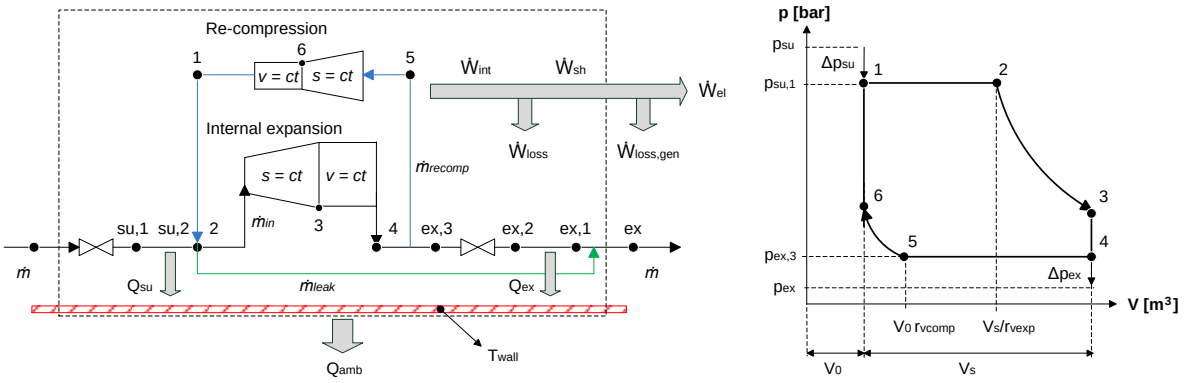


**Figure 2:** Scheme of the model and associated p-V diagram.

### 3.4 Gear pump model

The evaporation pressure ($p_{su}$), input of the expander model, is strongly correlated to the pump speed. These two quantities are independent input variable of the model, when the expander behavior is simulated without considering its integration into the ORC circuit, but in the real operation of the system, they are not. In order to simulate the changing of the fluid in the real operation of the system this relationship must be defined. Thus, a simplified semi-empirical model of the pump has been developed in order to relate the pump speed (i.e. the pump feed frequency) with the expander inlet pressure.

The characteristic curves of the volumetric pump are defined by the trend of the pressure head as function of the volume flow rate for different feed frequency. The actual operating point of the pump is determined by crossing the characteristic curve of the pump with the resistance characteristic of the circuit. The resistance of the system is influenced by the number of the activated resistive loads dissipating the electric power generated by the expander. An increasing of the activated loads leads to a minor resistance of the circuit, thus to higher values of pressure difference for a given value of the

volume flow rate. For the micro-ORC system of the case study, both these characteristic curves have been traced by interpolating the experimental data (collected testing the system with R134a). The resulting curves are reported in Figure 3.

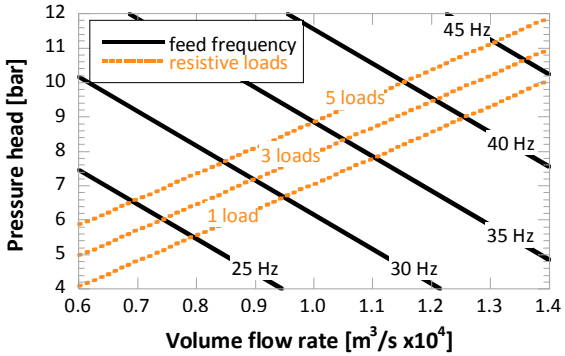


**Figure 3:** Experimental characteristic curves of the pump and resistance curves of the system.

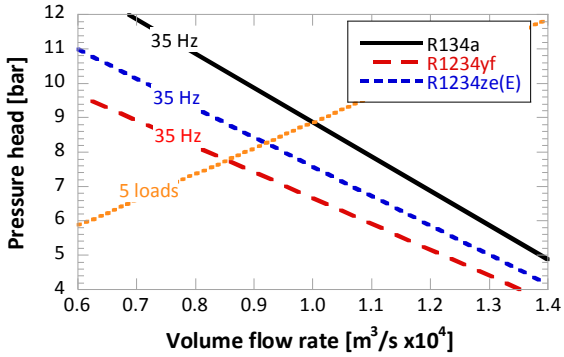


**Figure 4:** Characteristic curve of the pump obtained for the analyzed working fluids.

**Table 2:** Parameters of the integrated model.

Corrected heat transfer parameters for the expander model

| Parameters | Fluids | | |
|---|---|---|---|
| | R134a | R1234yf | R1234ze(E) |
| $(AU)_{su,ref}$ [W/K x $10^5$] | 5.65 | 6.38 | 6.53 |
| $(AU)_{ex,ref}$ [W/K x $10^5$] | 9.23 | 10.19 | 10.13 |

Parameters values for the pump model

| Parameter | Value |
|---|---|
| $c_1$ | 5.65 x $10^2$ |
| $c_2$ | 5.24 x $10^8$ |
| $V_{cc}$ | 64.7 ($cm^3$) |

### 3.5 Correction of the slope of the pump characteristic curve

To a first approximation, the volume flow rate actually elaborated by the pump, $\dot{V}$, is equal to the difference between the theoretical volume flow rate that the pump could elaborate ($\dot{V}_{th}$) and the leakage flow rate lost through the meatus.

$$\dot{V} = \dot{V}_{th} - \dot{V}_{leak} \tag{5}$$

Due to the pressure difference, $\Delta p$, between inlet and outlet of the pump, a leakage occurs through its internal clearance, in particular, through the space between the tips of the gear teeth and the cavity wall. Poiseuilles law for laminar flow is here used to evaluate the leakage flow, $\dot{V}_{leak}$, through the meatus, as function of the viscosity of the fluid, $\mu$, of the meatus geometry and of the pressure difference between inlet and outlet, according to the following equation:

$$\dot{V}_{leak} = \frac{b \cdot h^3 \cdot \Delta p}{12 \cdot \mu \cdot l} \tag{6}$$

where $h$ is the meatus height, $l$ the length and $b$ the width. The theoretical volume flow rate is equal to the cubic capacity ($V_{cc}$) multiplied by the rotational speed ($N_{pump}$), which corresponds also to the value of the volume flow rate at null pressure head.

$$\dot{V}_{th} = V_{cc} \cdot \frac{N_{pump}}{60} = \dot{V}(\Delta p = 0) \tag{7}$$

The set of equations (5–7) define the linear dependence of the pressure head $\Delta p$ on the volume flow rate. Indeed, being constant the geometrical quantities, the expression of the pressure head can be written as:

$$\Delta p = (c_1 \cdot N_{pump} - \dot{V} \cdot c_2) \cdot \mu \tag{8}$$

where $c_1$ and $c_2$ are constant (with $c_1 = c_2 \cdot V_{cc} / 60$ and $c_2 = 12 \cdot l/b/h^3$), experimentally determined by interpolating the data collected during the test performed on R134a. Once the rotational speed is set,

$\dot{V}$ is only affected by the fluid viscosity. Therefore, the effect of the change of the working fluid on the pump characteristic curve is a variation of the curve slope, as shown in Figure 4. For given values of the volume flow rate and the rotational speed, a fluid with a lower viscosity achieves lower value of pressure head throughout the pump. The viscosity of the fluid has been evaluated, for all the analyzed fluids, in the reference condition of saturated liquid at 20 °C. The constant parameters of equation (8) are reported in Table 2. Once the elaborated volume flow rate, $\dot{V}$, is evaluated, it is possible to determine the fluid mass flow rate, $\dot{m}$, input to the expander model, assuming the fluid density in the reference condition of saturated liquid at 20 °C.

## 4. RESULTS AND COMPARISON

The above described integrated model can be used to simulate the behavior of the expander in different operating conditions of the micro-ORC system, when changing the working fluid. A parametric analysis has been performed setting the expander inlet temperature equal to 75 °C, the condensation temperature equal to 20 °C, 5 activated loads, and varying the feed pump frequency between 25 and 45 Hz, for each analyzed fluid. The results are shown in the form of performance maps of the electric power output (Figure 5) and electric isentropic efficiency (Figure 6), as function of the mass flow rate and the pressure ratio, respectively. The results highlight that maximum electric power output, for the given operating conditions, at the same mass flow rate, is achieved with R134a, followed by R1234ze(E) and then by R1234yf. At the design value of the mass flow rate, equal to 0.15 kg/s, the electric power decreases by 17 % when using R1234yf and by 12 % in case of R1234ze(E). Indeed, the comparative analysis identifies in the R1234ze(E) the best candidate to maximize the electric power output and minimize the environmental impact at the same time. The derating of the expander performance when substituting R134a with the low GWP fluids are due to several factors of influence as: lower viscosity of the HFO fluids (mainly affecting the pump performance), lower density (affecting the mass flow rate elaborated by the expander), different saturation pressures (affecting the enthalpy drop through the expander) and higher values of the heat transfer parameters, see Table 2 (resulting in higher ambient heat loss).

The increase of the ambient heat loss, due to the use of HFOs as working fluids, entails the decrease of the maximum achievable isentropic electric efficiency. The maximum isentropic electric efficiency achievable with R1234yf decreases by 11 % compared to R134a value, while the maximum isentropic efficiency achievable with R1234ze(E) decreases by 17 %. Being different the evaporation pressure and the condensation pressure values of the fluids at the same hot and cold source temperatures, the peaks of the isentropic electric efficiency curves are not aligned at the same pressure ratio as visible in Figure 6.

The built-in volume ratio parameter ($r_{v,exp}$) has been optimized for the case study, for each analyzed fluid, for given reference conditions corresponding to the design operating point. The design point is defined as follows: expander inlet temperature equal to 75 °C, condensation temperature equal to 20 °C, 5 activated loads and 35 Hz of feed pump frequency. In order to evaluate the effect of the built-in volume ratio over the mass flow rate elaborated by the expander, in this study, the expander shaft speed has been set, so that the mass flow rate can become an output of the model, in place of the shaft speed. The trend of the electric power output (Figure 7), the specific work and the elaborated mass flow rate (Figure 8) are plotted against the intake stroke ratio, for a value of the expander shaft speed equal to 700 rpm. The intake stoke ratio, named α, represents the piston relative swept volume at the moment when the intake valve closes. Thus α is defined as the inverse of the built-in volume ratio.

$$\alpha = \frac{V_2 - V_1}{V_s} = \frac{1}{r_{v,exp}} \tag{9}$$

The bell curve of the electric power results by the combination of the opposite trends of the specific work and the elaborated mass flow rate; indeed, the electric power is proportional to the product between the latter. The specific work decreases when α increases, because of the under-expansion losses; conversely, the elaborated mass flow rate increases with α, because the more inlet port closes later, the more the fluid has time to enters into the cylinder. Maximum of electric power output is observed for $\alpha$ around 0.37, for the analyzed fluids. The actual value of $\alpha$ is close to 0.69, as obtained in previous work of the Authors (Bianchi *et al.*, 2019b), by the calibration of the parameters of the

expander model (see $r_{v,exp}$ value in Table 1). Figure 7 shows that the optimization of the built-in volume ratio for the case study could increases up to 43% the generated electric power, compared to actual value.

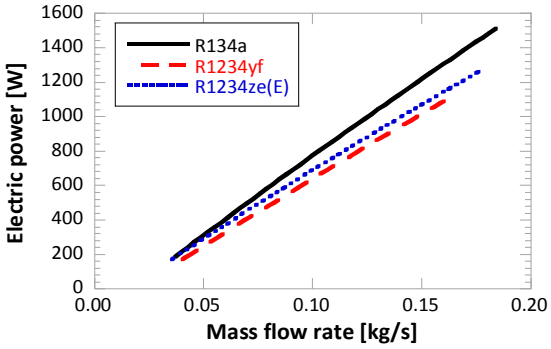


**Figure 5:** Trend of the electric power as function of the mass flow rate.

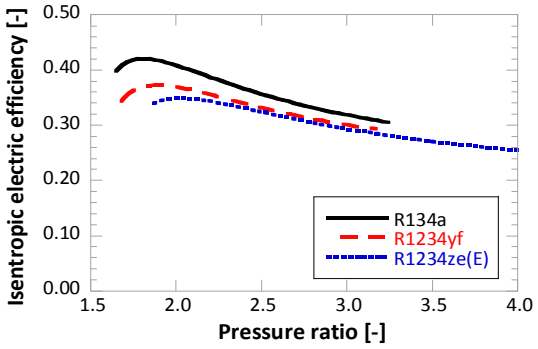


**Figure 6:** Trend of the isentropic efficiency as function of the pressure ratio.

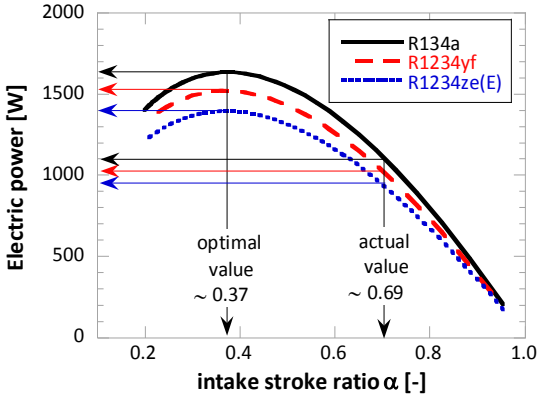


**Figure 7:** Trend of the electric power as function of the intake stroke ratio.

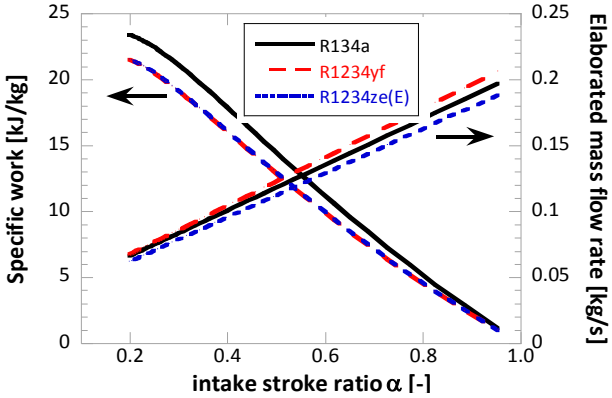


**Figure 8:** Specific work and elaborated mass flow rate trends as function of the intake stroke ratio.

## 5. CONCLUSION

The purpose of this work was to investigate the performance of a reciprocating piston expander, integrated into a micro-ORC system, when changing the working fluid (R134a) with low global warming potential alternatives (R1234yf and R1234ze(E)). A previously calibrated and validated semi-empirical model has been adapted to accommodate this change. A semi-empirical model of the gear pump, calibrated over the experimental data, has been presented, with the aim of integrating it with the expander model to reproduce its real operation into the actual ORC cycle. The results highlight that the expander electric power output, compared to the original R134a achieved value, decreases by 17 % when using R1234yf and by 12 % in case of R1234ze(E). A decrease in the maximum isentropic electric efficiency value is observed too. Among selected alternative fluids, the comparative analysis identifies in the R1234ze(E) the best candidate to maximize the expander electric power output while minimizing the environmental impact. The optimization of the built-in volume ratio could lead to an increase of the electric power output of 42 % when using R134a, of 43 % when using R1234yf and R1234ze(E).

## REFERENCES

Bell, I.H., Wronski, J., Quoilin, S., Lemort, V., 2014, Pure and pseudo-pure fluid thermophysical property evaluation and the open-source thermophysical property library CoolProp, *Ind. Eng. Chem. Res.*, vol. 53, no. 6: 249-508.

Bianchi, M., Branchini, L., Cesari, N., De Pascale, A., Melino, F., Ottaviano, S., Pinelli, M., Spina, P.R., Suman, A., 2019, Experimental analysis of a mirco-ORC driven by piston expander for low-grade heat recovery, *Appl. Therm. Eng.*, vol. 148, p. 1278-1291.

Bianchi, M., Branchini, L., De Pascale, A., Melino, F., Ottaviano, S., Peretto, A., Torricelli, N., 2019, Performance prediction of a reciprocating piston expander with semi-empirical models, *Energy Procedia*, vol, p. 1737–1743.

Dumont, O., Dickes, R., Lemort, V., 2017, Extrapolability and limitations of a semi-empirical model for the simulation of volumetric expanders, *Energy procedia*, vol. 129, p. 315-322.

Glavatskaya, Y., Podevin, P., Lemort, V., Shonda, O, Descombes, G., 2012, Reciprocating Expander for an Exhaust Heat Recovery Rankine Cycle for a Passenger Car Application, *Energies*, vol. 5, p. 1751-1765.

Giuffrida, A., 2014, Modelling the performance of a scroll expander for small organic Rankine cycles when changing the working fluid, *Appl. Therm. Eng.*, vol. 70, p. 1040-1049.

Le, V. L., Feidt, M., Kheiri, A., Pelloux-Prayer, S., 2014, Performance optimization of low-temperature power generation by supercritical ORCs (organic Rankine cycles) using low GWP (global warming potential) working fluids, *Energy*, vol. 67, p. 513-526.

Molés, F., Navarro-Esibrì, J., Peris, B., Mota-Babiloni, A., Mateu-Royo, C., 2017, R1234yf and R1234ze as alternatives to R134a in Organic Rankine Cycles for low temperature heat sources, *Energy Procedia*, vol. 142, p. 1192-1198.

Qiu, G., 2012, Selection of working fluids for micro-CHP systems with ORC, *Renewable Energy*, vol. 48, p. 565-570.

Quoilin, S., Van Den Broek, M., Declaye, S., Dewallef, P., Lemort, V., 2013, Techno-economic survey of Organic Rankine Cycle (ORC) systems, *Renewable Sustainable Energy Rev*., vol. 22, p. 168–186.

Yamada, N., Mohamad, M. N. A., Kien, T. T., 2012, Study on thermal efficiency of low- to medium-temperature organic Rankine cycles using HFO−1234yf, *Renewable Energy*, vol. 41, p. 368-375.

## NOMENCLATURE

**Symbols**

| | |
|---|---|
| $AU$ | Overall heat transfer coefficient (W/K) |
| $b$ | Meatus thickness (m) |
| $c_p$ | Specific heat at constant pressure (J/kg/K) |
| $f$ | Frequency (Hz) |
| $h$ | Meatus height (m) |
| $\dot{m}$ | Mass flow rate (kg/s) |
| $l$ | Meatus width (m) |
| $L$ | Characteristic length (m) |
| $N$ | Rotational speed (rpm) |
| $n$ | Number (-) |
| $Nu$ | Nusselt number (-) |
| $p$ | Pressure (Pa) |
| $Pr$ | Prandlt number(-) |
| $\dot{Q}$ | Heat flow (W) |
| $Re$ | Reynolds number (-) |
| $r_v$ | Volumetric ratio (-) |
| $T$ | Temperature (°C) |
| $U$ | Global heat transfer coefficient (W/m$^2$/K) |
| $V$ | Volume (m$^3$) |
| $\dot{V}$ | Volume flow rate (m$^3$/s) |
| $\dot{W}$ | Power (W) |

**Greek letters**

| | |
|---|---|
| $\alpha$ | Intake stroke ratio (-) |
| $\lambda$ | Conductive heat transfer coefficient (W·m/K) |
| $\Delta$ | Difference (-) |
| $\rho$ | Density (kg/m$^3$) |
| $\mu$ | Viscosity (Pa·s) |

**Acronyms**

| | |
|---|---|
| *CFC* | Chlorofluorocarbon |
| *GWP* | Global warming potential |
| *HCFC* | Hydrochlorofluorocarbon |
| *HFO* | Hydrofluoroolefine |
| *ORC* | Organic Rankine Cycle |

**Subscripts**

| | |
|---|---|
| *amb* | Ambient |
| *cc* | Cubic capacity |
| *el* | Electric |
| *ex* | Exhaust |
| *exp* | Expander |
| *fluid* | Fluid |
| *gen* | Generator |
| *H2O hot in* | Water at the evaporator inlet |
| *H2O cooling in* | Water at the condenser inlet |
| *int* | Internal |
| *leak* | Leakage |
| *loads* | Loads |
| *loss* | Loss |
| *pump* | Pump |
| *recomp* | Re-compression |
| *ref* | Reference |
| *R134a* | R134a |
| *sh* | Shaft |
| *su* | Supply |
| *s* | Swept |
| *th* | Theoretical |
| *wall* | Wall |
| *0* | Clearance |